ISSN: 0974-5823 Vol. 7 No. 2 February, 2022

International Journal of Mechanical Engineering

Synthesis and Structural Characterization of Zn-Mg ferrite doped with Samarium

Shailndra Singh[1*] and Sahi Ram[2]

Material Science Laboratory, Department of Physics, J. N. V. University Jodhpur

ABSTRACT.

The high temperature solid sate reaction approach was used to successfully synthesize $Zn_{0.5}Mg_{0.5}Fe_{2-x}Sm_xO_4$ (where x = 0.02, 0.06, 0.10) ferrite nanoparticles. The development of spinel phase in ferrite samples, together with secondary phases and space group Fd3m, is confirmed by XRD patterns. Crystallite sizes dropped as Sm^{3+} ion concentration rise, whereas lattice constant increased. The production of single phase cubic spinel is also seen in the FTIR spectra of the ferrite samples under examination, with two significant absorption bands ν1 and ν2 attributed to random variation of cations in the spinel structure. The cation distribution is influenced by the technique of production and the type of the additions, which affects the structural properties.

Keyword:- Nanoparticles, Crystallite, Sm^{3+} ion, FTIR spectra, technique

INTRODUCTION

Due to their magnetic characteristics, high electrical resistivity, and low eddy current and dielectric loss, spinel ferrites are a technologically important type of magnetic oxides [1]. These characteristics of ferrites are substantially influenced by their chemical composition, cation distribution, manufacturing process, and structure [2, 3]. Ferrite's microstructure, porosity, and grain size all have a role in determining ac susceptibility [4]. The occurrence of several types of domains in magnetic materials, such as multi-domain (MD), single domain (SD), and super-paramagnetic (SP) structure, is investigated in studies on temperature fluctuation of ac susceptibility [5]. The domain structure of spinel ferrites changes when additives are substituted [6, 7]. Because it interacts with 3d electrons of transition metals, rare-earth elements, which have their 4f orbital completely screened by 5s and 5p orbital's, play a crucial role in determining the electrical and magnetic characteristics of ferrites [8]. The impact of simultaneous replacement of divalent and trivalent metal ions on the magnetic characteristics of ferrites was fascinating to investigate. The effect of Sm^{3+} substitution on the structural and magnetic characteristics of Mg–Zn ferrite is discussed in this paper.

The materials were sintered at 1180°C and a series of $Zn_{0.5}Mg_{0.5}Fe_{2-x}Sm_xO_4$ (where x = 0.02, 0.06, 0.10) ferrite nanoparticles were produced utilising a solid state reaction approach. For characterisation, X-Ray diffraction (XRD) and Fourier Transform Infrared Spectroscopy (FTIR) were used.

EXPERIMENTAL

The spinel ferrite samples of Zn-Mg ferrite ($Zn_{0.5}Mg_{0.5}Sm_xFe_{2-x}O_4$) were prepared by a conventional solid state reaction method. Each step from mixing to sintering has been controlled carefully to get the high density product. The stoichiometric mixture of raw oxides, ZnO (zinc oxide), MgO (magnesium oxide), Fe_2O_3 (iron oxide), Sm_2O_3 (samarium oxide) of high purity (99.999% pure) obtained from Sigma Eldrich were weighed on a single pan electronic balance with accuracy 0.0001 and mixed thoroughly to get the desired product. These oxides were grinded in agate-mortar in a wet medium (acetone) for 2 hours and calcined at 600°C for 8 hours in a Alumina crucible in air atmosphere [9].

The calcined lump was again grinded for 2 hours and re-calcined at 800°C for 8 hours in Alumina crucible. The process of firing and grinding was repeated for a number of times whenever the homogenous mixer not found. The resulting mixture was grinded again and compressed into cylindrical pellets by applying pressure around 5tones/cm^2 using hydraulic press. These pellets were completely sintered at 1180°C for 2 hour. A flow chart diagram for the whole process of formation of the pure $Zn_{0.5}Mg_{0.5}Sm_xFe_{2-x}O_4$ compound is shown in figure 1.

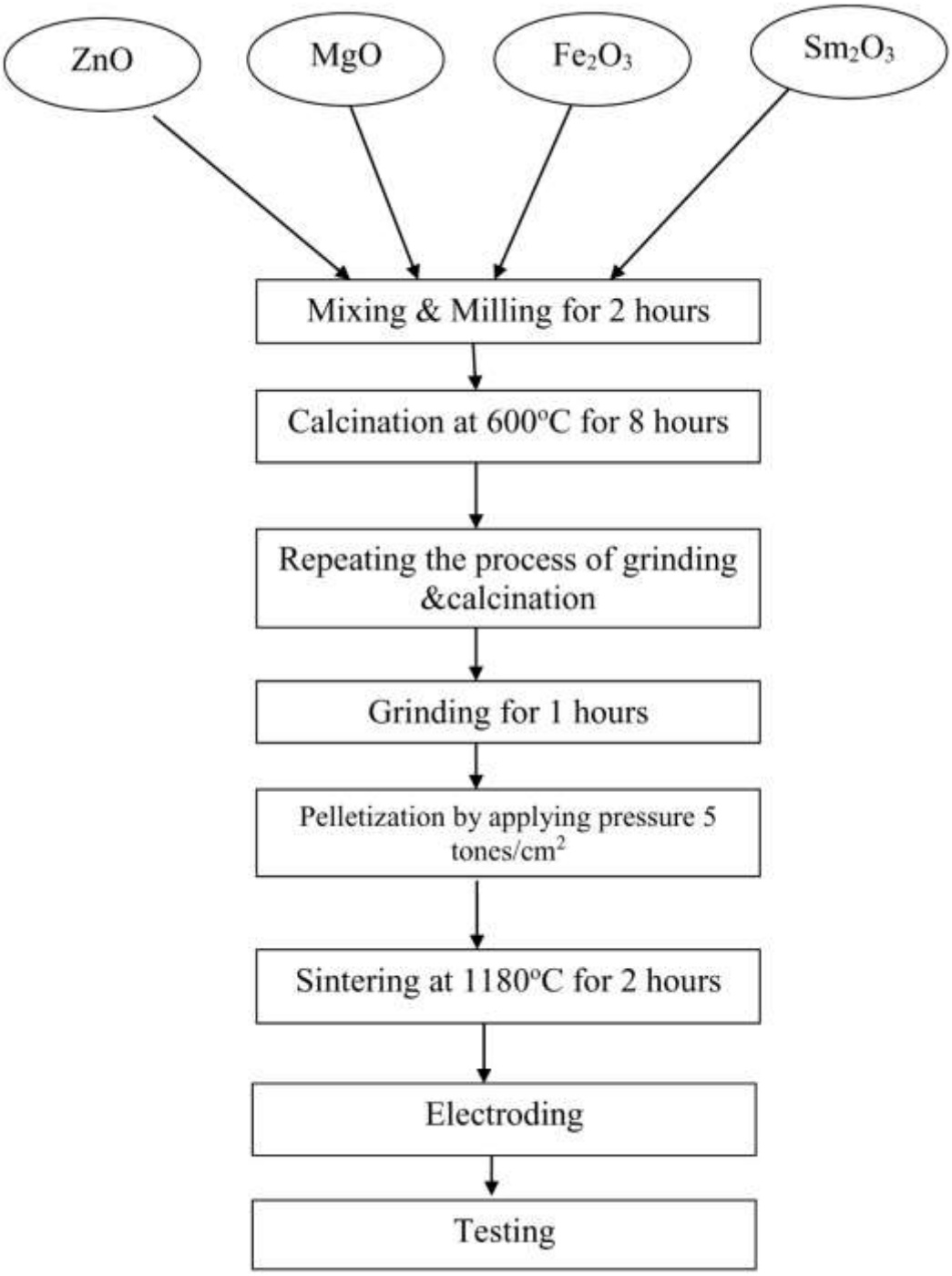

Figure 1: A flow chart diagram for the formation of Sm modified $Zn_{0.5}Mg_{0.5}Fe_2O_4$ ferrite.

On a PANalytical X'pert Pro MPD diffractometer of Cu-K radiation, X-ray diffraction data were gathered at room temperature at a 2^o/min scanning rate from 10^o to 80^o ranges of 2θ. The crystallite size, lattice constant, and other parameters were computed. FTIR interferometer IR prestige-2 was used to examine the inherent vibrational frequency of the tetrahedral and octahedral sites of the spinel structure in the region of 400 to 4000 cm^{-1}.

RESULT AND DISCUSSION

To analyses the structural phase of $Zn_{0.5}Mg_{0.5}Fe_{2-x}Sm_xO_4$ (where x = 0.02, 0.06, 0.10) ferrite samples, X-ray diffraction investigations were done, and the resulting XRD patterns are shown in Figure 2. The cubic spinel structure with space group Fd3m is shown by the XRD patterns. The diffraction planes were evaluated using "Fullprof" software, and the planes were indexed as (111), (220), (311), (400), (422), (511), and (440), which correspond to the prior studies [10]. The presence of ultrafine particles in the samples is responsible for the widening and low intensity of diffraction peaks.

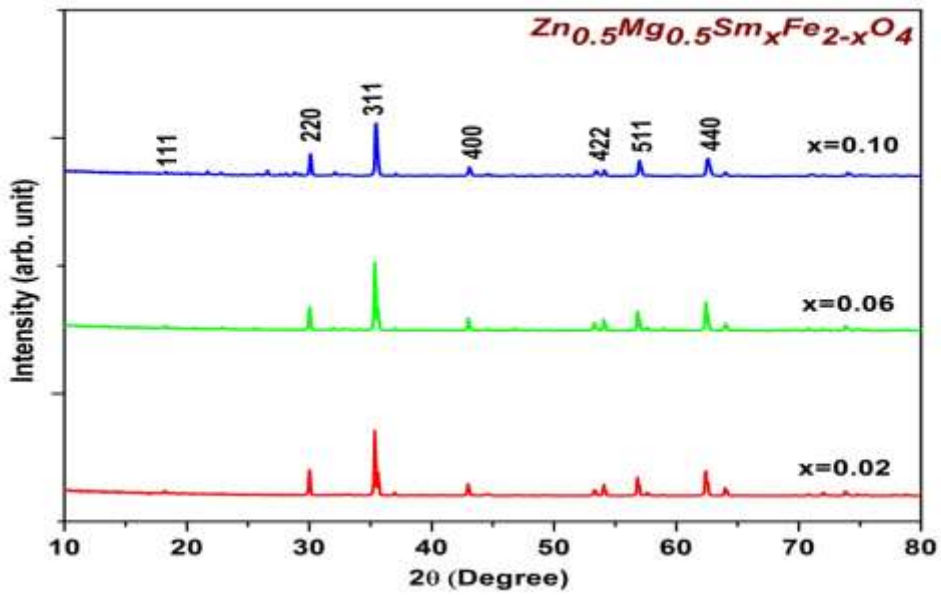

Figure: 2 X-ray powder diffraction pattern of $Zn_{0.5}Mg_{0.5}Sm_xFe_{2-x}O_4$ (where x=0.02, 0.06, 0.10)

The following relationships were used to compute the structural and micro structural parameters. The average lattice constant values (a) were calculated using the Bragg's diffraction [11] condition and two values of the most intense peaks.

$$a = \frac{\lambda\sqrt{h^2+k^2+l^2}}{2sin\theta} \qquad \text{---------- (1)}$$

The average crystallite sizes are calculated with full width at half maximum of most intense peaks using Debye–Sherrer's [11] equation, given by

$$t = \frac{K\lambda}{\beta cos\theta} \qquad \text{---------- (2)}$$

Where *K* is shape factor taken as 0.89, λ is the X-ray wavelength used and β is full width at half maximum intensity taking into account of instrumental broadening.

The X-ray density [11] has been calculated using the relation

$$\rho_x = \frac{8M}{N_A a^3} \qquad \text{---------- (3)}$$

Where *M* is molecular weight of the ferrite sample, N_A is Avogadro's number and *a* is an experimental lattice constant.

The lattice strain was estimated from the following derived relation modifying the Williamson and Hall equation [12]

$$\eta = \frac{2d|K-1|}{t} \qquad \text{---------- (4)}$$

Where d is lattice spacing for (311) planes, *t* is average crystallite size and *K* (0.89) is shape factor.

Table.1 summarizes the computed values of lattice constant (a), crystallite size (t), X-ray density (x), and lattice strain (η). The values of the lattice parameter are similar to those reported for $Zn_{0.5}Mg_{0.5}Fe_2O_4$ [13] and range from 8.4071 to 8.4112. The lattice

constant rises monotonically with the replacement of Sm^{3+}, which can be attributed to Fe^{3+} (0.69Å) having a lower ionic radius than Sm^{3+} (1.09Å). Other spinel ferrites have been shown to have comparable properties [13, 14, 15]. With an increase in Sm^{3+} ion concentration, the crystallite size decreases, resulting in a rise in lattice strain. Figure 2 shows how changes in lattice constant and crystallite size follow Vegard's rule [16].

Table 1: Variation of other X-Ray parameters as change the Sm^{+3} concentrations

Concentrations	Lattice Constant (Å)	Crystallite Size(nm)	X-Ray Density $\rho_x(g/cm^3)$	Lattice Strain $\eta(\times 10^{-2})$
X=0.02	8.4071	51	4.926	1.093
X=0.06	8.4086	48.86	4.928	1.138
X=0.10	8.4112	43.42	4.932	1.280

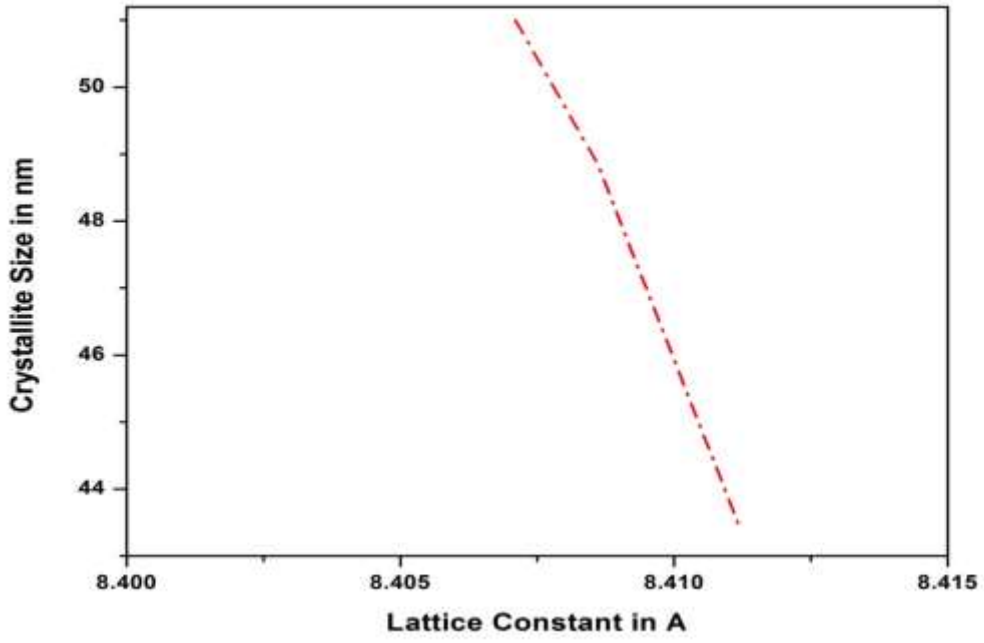

Figure 2: Change in lattice constant with crystallite size

The density of the experiment increased as the concentration of Sm^{3+} ions increased. Despite increasing the lattice constant, the variation in experimental density is dependent on the ferrite molecular weight. The replacement of Sm^{3+} with a high atomic mass significantly increased the molecular weight of ferrite in this research, resulting in increased density.

The structural fluctuations and spinel phase of ferrite systems have been observed using Fourier transform infrared spectroscopy. The two vibrational bands are the typical bands of cubic spinel structure [17], one with a greater vibrational frequency (v1) in the range of ~565 cm^{-1} and the other with a lower vibrational frequency (v2) in the range of 451.25 cm^{-1}- 452.34 cm^{-1}. Fe^{3+}- O^{2-} stretching vibrations at the tetrahedral site (A) have a greater vibrational frequency (v1) while Fe^{3+}- O^{2-} stretching vibrations at the octahedral site (B) have a lower vibrational frequency (v2). (B).Figure 3 shows the FTIR spectra of $Zn_{0.5}Mg_{0.5}Fe_{2-x}Sm_xO_4$ (where x = 0.02, 0.06, 0.10).

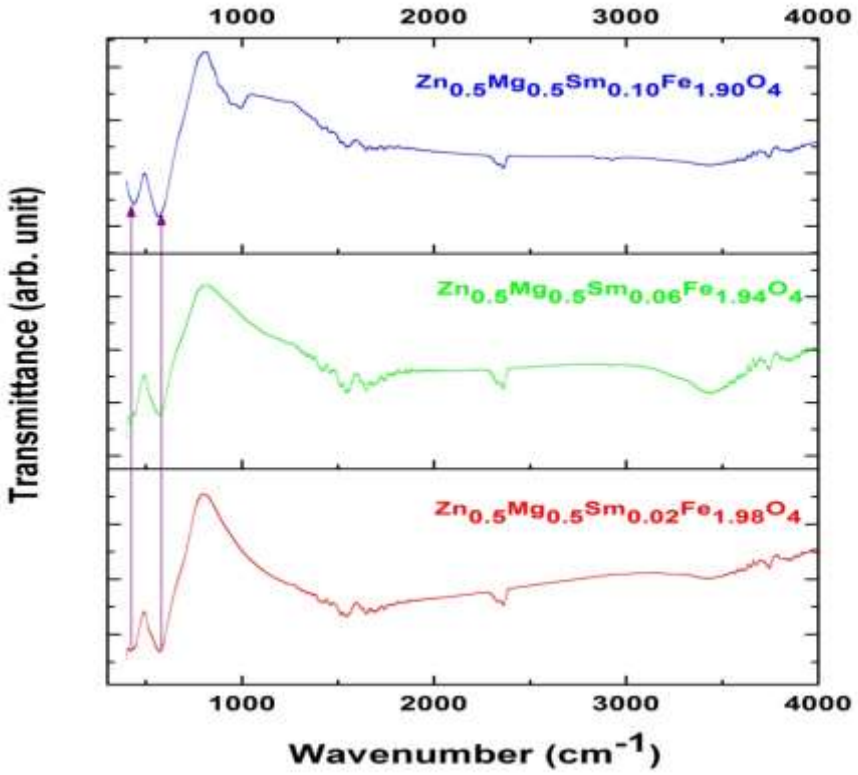

Figure: 3 FT-IR spectra of $Zn_{0.5}Mg_{0.5}Sm_xFe_{2-x}O_4$ (where x=0.0, 0.02, 0.06, 0.10)

The force constants has been calculated using the formula

$K = 4\pi^2c^2\nu^2\mu$ ---------- (5)

Where c is the light speed (~2.99 x 10^{10} cm/s), ν is the vibration frequency of the A- and B- sites and μ is the reduced mass of the Fe^{3+} and O^{2-} ions (~2.60 1x 10^{-23} g).

Table 2: Tetrahedral, octahedral vibrational frequencies (ν1 and ν2) and force constant (K_t and K_o)

x	ν1 (cm^{-1})	ν2 (cm^{-1})	K_t(dyne/cm)	K_o(dyne/cm)
0.02	564.8	451.25	2.945E-05	1.8799E-05
0.06	565.28	451.9	2.9501E-05	1.8853E-05
0.10	566.92	452.34	2.9672E-05	1.889E-05

The band frequency ν2 rises and broadens with Sm^{+3} concentration, however ν1 does not vary significantly and just a little broadening is seen, which may be due to the substitution of Fe^{3+} ions on octahedral B-sites by Sm^{+3} ions. The observed increases in lattice constant [18] are supported by this. The declines in ν1 and ν2 in the current series are due to cation random distribution in tetrahedral (A) and octahedral (B) sites, which is contrary to their typical predilection. The hydroxyl group may be allocated to the wide band around 3700 cm-1, while the in-plane and out-plane of O–H vibration can be ascribed to the bands around 1550–1520 cm^{-1} and 2370-2350 cm^{-1}. The remaining bands are very certainly attributable to overtones or combinational frequencies.

CONCLUSION

The high temperature solid sate reaction approach was used to successfully synthesize $Zn_{0.5}Mg_{0.5}Fe_{2-x}Sm_xO_4$ (where x = 0.02, 0.06, 0.10) ferrite nanoparticles. The development of spinel phase in ferrite samples, together with secondary phases and space

group Fd3m, is confirmed by XRD patterns. Crystallite sizes dropped as Sm^{3+} ion concentration rise, whereas lattice characteristics increased. The production of single phase cubic spinel is also seen in the FTIR spectra of the ferrite samples under examination, with two substantial absorption bands ν1 and ν2 attributed to random variation of cations in the spinel structure. The cation distribution is influenced by the technique of production and the type of the additions, which affects the structural properties.

ACKNOWLEDGEMENT

Authors are thankful to Department of Physics J. N. V. University Jodhpur for providing the XRD facility. One of the authors Shailndra Singh is thankful to UGC for providing the UGC-BSR doctoral fellowship.

REFERENCES

1. M. Ishil, M. Nakahita, Yamanka, "Journal of Solid State Communication" 11 (1972) 209.
2. V.R.K. Murthy, S. Chitrashankar, K.V. Reddy, J. Shobanadri, "Indian Journal of Pure Applied Physics" 16 (1978) 79.
3. M.A. El Hiti, A.I. El Shora, Seoud, S.M. Hammed, J. Phase Transitions 56 (1995) 35.
4. A.Y. Lipare, P.N. Vasambekar, A.S. Vaingankar, "A.c. susceptibility study of CaCl2 doped copper–zinc ferrite system", Bulletin of Materials Science, 26 (5) (2003) 493–497.
5. C.P. Bean, "Journal of Applied Phycology, 26 (1955) 1981.
6. E. Rezlescu, N. Rezlescu, C. Pasnicu, M.L. Craus, D.D. Popa, "Journal of magnetism and magnetic materials, 215 (2000) 194.
7. C. Radhakrishnamurthy, R. Nagarajan, Bulletin of Materials Science 3 (1981) 217.
8. C.B. Kolekar, P.N. Kamble, A.S. Vaingankar, "Indian Journal of Pure Applied Physics" A68 (6) (1994) 529.
9. S. Singh and S. Ram "Structural and Dielectric Studies of $Zn_{0.5}Mg_{0.5}Pr_xFe_{2-x}O_4$ Ferrites" Vidyabharati International Interdisciplinary Research Journal (2021) 1823-1834.
10. Shailndra singh, S. K. Barbar and Sahi Ram "Synthesis and Characterization of Zn-Mg Ferrite" AIP Conf. Proc. 1953, (2018) 090023-1–090023-4.
11. R. P. Patil, S. D. Delekar, D. R.Mane, P. P. Hankare "Synthesis, structural and magnetic properties of different metal ion substituted nanocrystalline zinc ferrite" Results in Physics 39(2013)129-133.
12. Ch. Srinivas, B.V.Tirupanyam, S. S. Meena, S. M. Yusuf, Ch. SeshuBabu, K.S. Ramakrishna, D. M. Potukuchi, D. L. Sastry "Structural and magnetic characterization of co-precipitated $Ni_xZn_{1-x}Fe_2O_4$ ferrite nanoparticles" J. Magn. Magn. Mater 407 (2016) 135-141.
13. Anjali Verma, Ratnamala Chatterjee "Effect of zinc concentration on the structural, electrical and magnetic properties of Mn-Zn and Ni-Zn ferrites synthesized by the citrate precursor technique" J. Magn. Magn. Mater 306 (2006) 313-320.
14. M. Rahimi, P. Kameli, M. Ranjbar, H. Hajihashemi, H. Salamati "The effect of zinc doping on the structural and magnetic properties of $Ni_{1-x}Zn_xFe_2O_4$" J. Mater. Sci 48 (2013) 2969-2976.
15. Shailndra Singh, Sahi Ram and S. K. Barbar, "Structural and Dielectric Studies of Dy Doped Zn-Mg Ferrite", AIP Conference Proceedings, (2020), pp 080040-1–080040-4.
16. B. V. Tirupanyam, Ch. Srinivas, S. S. Meena, S. M. Yusuf, A. SatishKumar, D. L. Sastry, V. Seshubai "Investigation of structural and magnetic properties of co-precipitated Mn–Ni ferrite nanoparticles in the presence of α-Fe2O3 phase" J. Magn. Magn. Mater 392 (2015) 101–106.
17. P. Priyadharsini, A. Pradeep, P. Sambasiva Rao, G.Chandrasekaran "Structural, spectroscopic and magnetic studies of nanocrystalline Ni–Zn ferrites" Mater. Chem. Phys. 116(1) (2009) 207 213.
18. M. Rahimi, P. Kameli, M. Ranjbar, H. Hajihashemi, H. Salamati "The effect of zinc doping on the structural and magnetic properties of $Ni_xZn_{1-x}Fe_2O_4$" J. Mater. Sci. 48(2013) 2969–2976.